UNIVERSITY OF BIRMINGHAM

Research at Birmingham

Numerical simulation of combined adsorption desalination and cooling cycles with integrated evaporator/condenser

Youssef, Peter; Mahmoud, Saad; Al-Dadah, Raya

Link to publication on Research at Birmingham portal

Numerical Simulation of Combined Adsorption Desalination and Cooling Cycles with Integrated Evaporator/Condenser

Peter G. Youssef*, Saad M. Mahmoud, Raya K. AL-Dadah

Abstract- The availability of potable water and cooling are becoming increasingly important to ensure good sustainability and quality of life. In this work, a new multi-cycle adsorption desalination and cooling system using AQSOA-Z02 has been developed for high water production and cooling rates using renewable and waste heat sources. It consists of two 2-adsorber bed cycles linked with integrated evaporator/condenser, one cycle uses the integrated evaporator/condenser as evaporator (upper) and the second one uses it as a condenser (lower). In this system low condensing temperatures can be achieved using the cooling effect from the evaporator of the lower cycle and the integrated evaporator / condenser thus enhancing the system performance. Also, the adsorber beds of the upper and lower cycles are heated in series during the desorption process using the same heat source. This system can operate in three modes depending on the desalinated water and cooling capacity requirements. Results showed that the specific daily water production ranges from 6.64 to 15.4 m^3/tonne adsorbent/day while the cooling capacity reaches up 46.6 Rton/tonne adsorbent at evaporator temperature of 10°C. The new cycle offers potential of simultaneously producing large amounts of desalinated water and cooling capacity (at 10°C) compared to other cycles.

Keywords—Adsorption, AQSOA-Z02, Desalination, Cooling, Seawater.

I. INTRODUCTION

In the past few years, adsorption desalination technology has shown potential as a possible alternative for other desalination technologies [1, 2]. This technology can utilize low temperature waste heat to produce two useful effects; desalination and cooling. It can produce fresh water with low salinity of 10 ppm with minimal running cost of 0.2$/m^3 and CO_2 emissions of 0.6 kg/m^3 [3]. Adsorption desalination system is a thermodynamic cycle that consists of evaporation/adsorption and desorption/condensation processes where the adsorbent material adsorbs pure water vapour from the boiling seawater in the evaporator. This evaporation process is maintained by the adsorbing action of the adsorbent while external heat load in the form of flowing water in a coil, is used to stabilize the evaporation temperature. During this adsorption process, cooling fluid is needed to absorb the rejected heat of adsorption while in the desorption process, heating is applied to regenerate the adsorbed water vapour using waste heat or solar energy at low temperature. The desorbed water vapour is condensed in the condenser to produce potable water which is collected and pumped out of the condenser. Cooling effect is produced during the evaporation process which occurs at temperature ranging from 10-30°C [4].

Jun et al. [5, 6] studied theoretically and experimentally the effect of evaporator temperature relative to cooling water temperature on the performance of the cycle where cooling water temperature is the same for adsorbing bed and condenser. The cycle was studied for various evaporator temperatures higher, equal and lower than that of the cooling water. Results showed that when the evaporator temperature is below the cooling water temperature, the water production rate increases as the evaporator temperature increases while the energy consumption decreases. However, when the evaporator temperature is equal or higher than the cooling water temperature, the water production and energy consumption are not affected by the evaporator temperature.

*P. G. Youssef is a PhD student at University of Birmingham, UK (phone: +44-0121-4143513; fax: +44-0121-4143598; e-mail: pgy348@ bham.ac.uk).

Thu et al. [7], have studied experimentally the performance of a *silica gel* adsorption desalination system that operates on either two or four bed configurations. Water production, cycle time and performance ratio were investigated at different heat source temperatures and constant heat sink temperature. Experimental results showed that at low heat source temperature, a longer cycle time is required for the production of maximum amount of fresh water. Measurements showed that maximum water production achieved was 10 m^3 per day per tonne of *silica gel* at a performance ratio of 0.61 in the case of operating the cycle with four bed master-slave configuration. A significant improvement in specific daily water production (SDWP) was achieved compared to the 2 bed configuration which resulted in 8.79 m^3/day per tonne of *silica gel*.

Ng et al. [8], have developed a mathematical model for a 4 bed adsorption system using *silica gel*/water pair to produce both cooling and desalinated fresh water. At different hot and chilled water temperatures, cycle performance was analyzed by calculating specific cooling power (SCP), SDWP, and overall conversion ratio (OCR). It was found that a *silica gel* adsorption system can produce 8 m^3/day and 51.6 Rton per tonne of *silica gel* when optimized for water production at evaporator temperature of 30°C or 3.8 m^3/day and 22 Rton per tonne of *silica gel* at evaporator temperature of 10°C. In addition, the cycle can reach a maximum OCR of 1.4. Ng et al. [9], carried experimental testing of the modeled cycle and results showed that chilled water at 7 to 10°C with a specific cooling capacity (SCC) of 25-35 Rton/tonne of *silica gel* can be produced in addition to a SDWP of 3-5 m^3 per tonne of *silica gel* per day while the OCR is about 0.8-1.1.

Youssef et al. [10], have numerically studied the effect of evaporator and condenser water temperature on the performance of a silica-gel 2-bed cycle. Simulation results showed that as the condenser temperature decreases and evaporator temperature increases, cycle water production and cooling effect increase. A

61 water production of 10 m^3/tonne adsorbent /day and cooling effect of 77 Rton/tonne of adsorbent were
62 achieved at condenser and evaporator water inlet temperatures of 10°C and 30°C, respectively.

63

64   Youssef et al. [11], have compared numerically the performance of a 2-bed adsorption cycle using
65 *AQSOA-Z02/*water pair with the same cycle using *silica-gel/*water. Effect of evaporator water temperature
66 on cycle performance in terms of SDWP and coefficient of performance (COP) was studied. Results
67 showed that *AQSOA-Z02* is better for chilled water temperatures below 20°C as 5.8 m^3 of fresh water per
68 day and 50.1 Rton of cooling can be produced compared to *silica-gel* that can produce only 2.8 m^3 of fresh
69 water per day and 17.2 Rton of cooling at the same operating conditions. However, silica-gel proved to be
70 superior above 20°C as it can reach SDWP of 8.4 m^3 and 62.4 Rton of cooling.
71   Alam et al. [12], have proposed an advanced adsorption refrigeration cycle consisting of 4 beds
72 comprising of two 2-bed adsorption refrigeration cycles, upper and lower. A mass recovery scheme is
73 applied between the beds in the upper and lower cycles in addition to heat recovery for the heating source
74 between the two cycles. The results of the mathematical model showed that SCP and coefficient of
75 performance (COP) reached 14.3 Rton/tonne adsorbent and 0.6 respectively compared to performance of
76 the 2-bed cycle which resulted in 5.95 Rton/tonne adsorbent and 0.35 for SCP and COP respectively at the
77 same regeneration temperature of 65°C and based on cycle time of 1200 sec. However, at hot source
78 temperatures above 70°C, the COP of the advanced cycle is lower than that of the 2-bed cycle but resulted
79 in higher cooling effect than two stage chiller. Also, the proposed system can be converted to two-stage
80 chiller mode to make it able to cover wider range of heat source temperatures for the production of
81 effective cooling.
82   Thu et al. [13], have developed an advanced 2-bed adsorption desalination cycle that contains an
83 integrated evaporator-condenser device for better heat transfer. Numerical simulations were used to predict
84 the performance of a *silica gel* cycle operating in a 2 bed mode. It was found that using this cycle
85 configuration increases the evaporator temperature and vapor pressure in the adsorber beds because of
86 recovery of condenser heat. Results showed that SDWP improved by 300% compared to the conventional
87 adsorption desalination cycle as it reached 26 m^3/day per tonne of *silica gel* instead of 8 m^3/day per tonne
88 of *silica gel*. Moreover, lower specific electricity consumption were achieved at 1.38 kWh/m^3 as pumping
89 power was reduced due to dispensing of evaporator and condenser cooling water circulations.
90   Table I compares various adsorption systems that were reported to produce desalination and cooling
91 where different parameters are shown including adsorbent material, system type, amount of water produced
92 per day and amount of cooling produced. From this comparison, it was found that the highest amount of
93 fresh water produced was 10 m^3/tonne adsorbent/day when *silica gel* RD type was used [7]. However, it
94 reached 26 m^3/tonne adsorbent/day when advanced *silica gel* A^{++} type [14] was used at high evaporator
95 temperature of 42°C (not suitable for cooling applications) in an advanced adsorption desalination cycle
96 [13]. For water desalination and cooling, a maximum of 10 m^3/tonne adsorbent/day of water was produced
97 with 77 Rton/tonne adsorbent of cooling [10] when *silica gel* RD type was used at 10°C condensing
98 temperature and at high evaporating temperature of 30°C. In case of cooling production at low evaporator
99 temperature, 10°C, a maximum of 53.7 Rton/tonne adsorbent of cooling and 6.2 m^3/tonne adsorbent/day of
100 water were produced when *AQSOA-Z02* was used [15]. Finally, the maximum reported cooling production
101 with no water desalination was 85.7 Rton/tonne adsorbent at 7°C evaporating temperature with silica-gel A
102 type used [16]. Unlike the work done by Youssef et al [10, 11], in this paper AQSOA-Z02 is investigated
103 firstly at different condenser water temperatures (10-30°C) then it is studied in a new cycle configuration
104 comprising of four beds, condenser, evaporator and integrated evaporator-condenser device. The advantage
105 of this new cycle is its ability to lower the condenser temperature which results in an increase in water
106 production while producing cooling effect at low evaporator temperature (<15°C). This proposed system
107 allows working at different combinations of operating temperatures for evaporator and condenser pair
108 which gives operation flexibility that permits outputting different proportions of desalinated water and
109 cooling.

110

TABLE I
PUBLISHED WORK ON ADSORPTION DESALINATION AND COOLING

Author	System used	Experiment/ Simulation	Adsorbent material	T_{hot}	SDWP (m^3/tonne ads. /day)	SCP (Rton/tonne ads.) @ Evap. temp. (^{o}C)
Thu et al. [7]	2 &4 Bed	Experiment	Silica-gel, type RD	85°C	8.79 - 10	0 @ 30°C
Ng et al. [8]	4-Bed mode	Simulation	Silica-gel, type RD	85°C	8	51.6 @ 30°C
Ng et al. [9]	2 & 4 Bed	Exp. & Sim.	Silica-gel, type RD	85°C	3-5	25-35 @ 10°C
Thu et al. [17]	2-Bed (heat recovery)	Experiment	Silica-gel, type RD	70°C	9.2	0 @ 30°C
Thu et al. [18]	2-Bed, Evap.-Cond. heat recovery	Experiment	Silica-gel, type A^{++}	85°C	13.46	0 @ 32°C
Mitra et al. [19]	4-Bed mode	Experiment	Silica-gel, type RD	85°C	2.4	18 @ 5.4^{o}C
Mitra et al. [20]	2-Stage	Experiment	Silica-gel, type RD	85°C	1	7.5 @ 15°C
Youssef et al. [10]	2-Bed mode	Simulation	Silica-gel, type RD	85°C	10	77 @ 30°C
Youssef et al. [15]	4-Bed mode	Simulation	AQSOA-Z02	85°C	6.2	53.7 @ 10°C
Akahira et al. [16]	4-Bed cascading	Simulation	Silica-gel, type A	85°C	-	85.7 @ 7°C
Alam et al. [12]	2-Stage	Simulation	Silica-gel	65°C	-	14.3 @ 10°C
Thu et al. [13]	2-Bed, Integrated Evap./Cond.	Simulation	Silica-gel, type A^{++}	85°C	26	0 @ 42°C

111

II. SYSTEM DESCRIPTION

Figure 1 show the conventional adsorption system which consists of 2 beds, evaporator and condenser. Figure 2 shows the configuration of the proposed system, which consists of 4 beds, 1 evaporator, 1 condenser and 1 integrated evaporator/condenser device. Basically, this system is comprising of two conventional adsorption cycles, upper and lower where each cycle has 2 adsorber beds and 2 heat exchangers, (evaporator and condenser). The evaporator of the upper cycle and the condenser of the lower cycle are integrated together into one device which is the linkage between the upper and lower cycles. In the integrated evaporator/condenser device there are three streams of heat exchanging fluids which are supplied seawater, evaporator chilled water and condensing water vapor. Two of these streams are rejecting heat which are condensing water vapor and chilled water while seawater evaporation is the heat absorbing stream. Each cycle, upper and lower operates at 2 bed configuration with periods of switching between adsorption and desorption phases when evaporator and condenser are not connected to any of the beds. In addition, water vapor flows in both upper and lower cycles independently from each other. For better utilization of the available heat source, heat recovery between upper and lower desorbing beds is applied. In this case, the hot water that comes out of the desorbing bed in the upper cycle is fed again to the desorbing bed in lower cycle, Fig. 3.

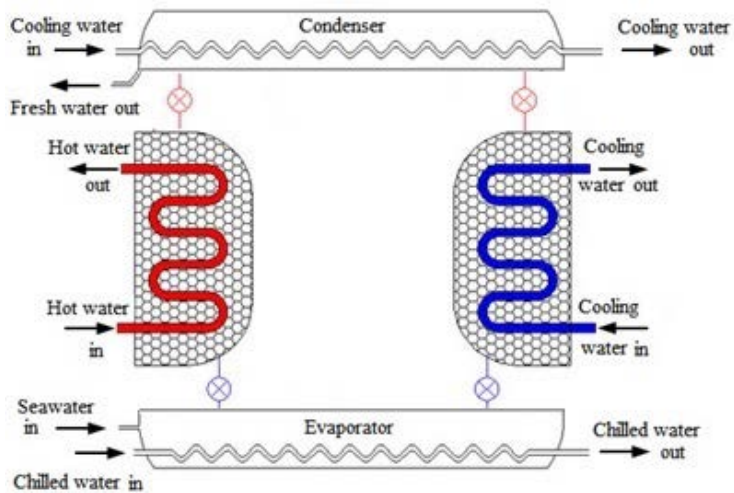128

129   Fig. 1 Schematic diagram of the conventional 2-bed adsorption system

130

131

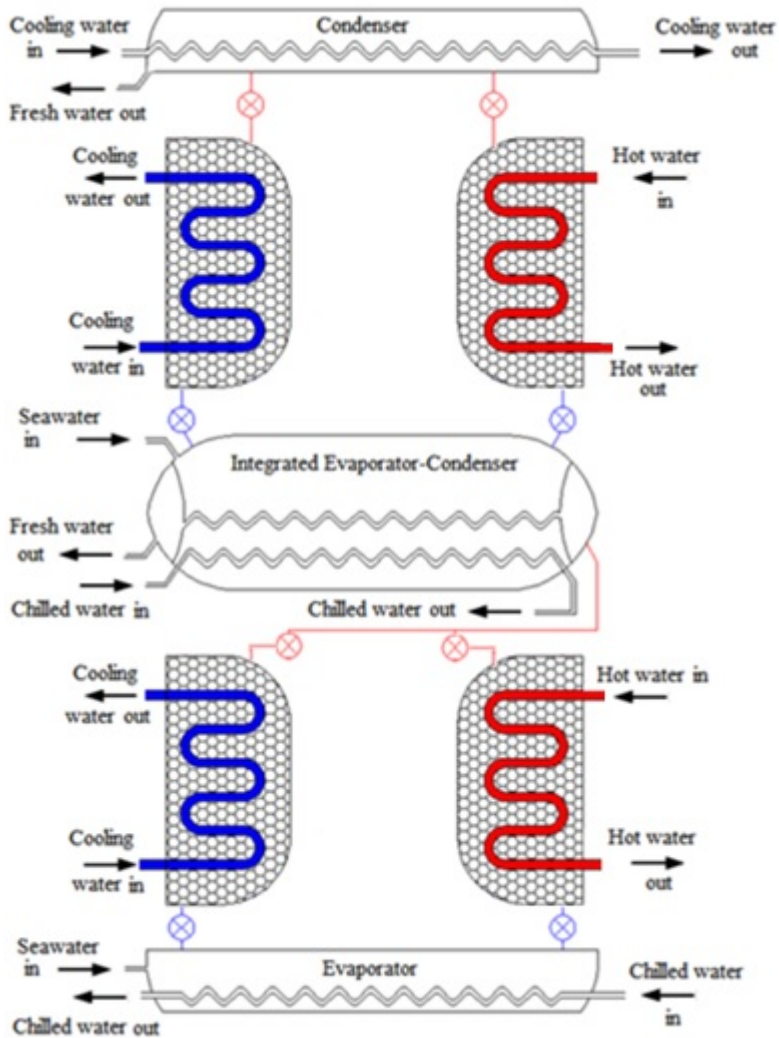132   Fig. 2 Schematic diagram of a multi-cycle adsorption desalination & cooling system with integrated
133   evaporator/condenser

Three different operating modes are suggested for this cycle. In all of these modes, fresh water is produced from two sources; one comes from upper condenser and the other one from the condenser part of the integrated evaporator/condenser device. Cooling is produced from the evaporators when chilled water is passes through them. In mode 'A', (fig. 3-a), no chilled water is fed into the integrated evaporator/condenser but in the lower evaporator there is flow of chilled water for cooling to be produced from lower cycle only. In mode 'B', (fig. 3-b), chilled water is fed into the evaporator part of the integrated evaporator/condenser for the upper cycle to produce cooling effect. At the same time, lower evaporator cold water output is fed to upper condenser so lower temperature in the upper condenser is achieved and two water production sources still exist. Finally, in mode 'C', (fig. 3-c) no cooling output is obtained as this mode operates similar to mode 'B' but no chilled water is fed into the integrated evaporator/condenser device. A summary of cycle outputs at these operating modes is presented in table II.

TABLE II
SYSTEM OUTPUTS AT DIFFERENT OPERATING MODES

Output Source / Operating Mode	Upper Cycle	Integrated Evaporator / Condenser		Lower Cycle
	Condenser			Evaporator
Mode 'A'	Fresh water	No Cooling	Fresh water	Cooling
Mode 'B'	Fresh water	Cooling	Fresh water	No Cooling
Mode 'C'	Fresh water	No Cooling	Fresh water	No Cooling
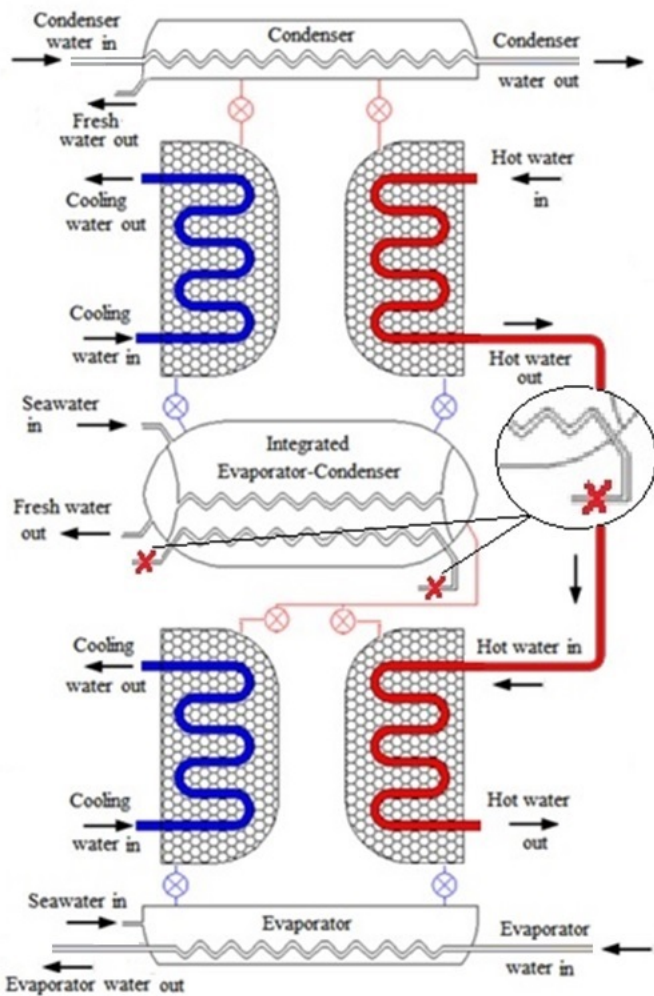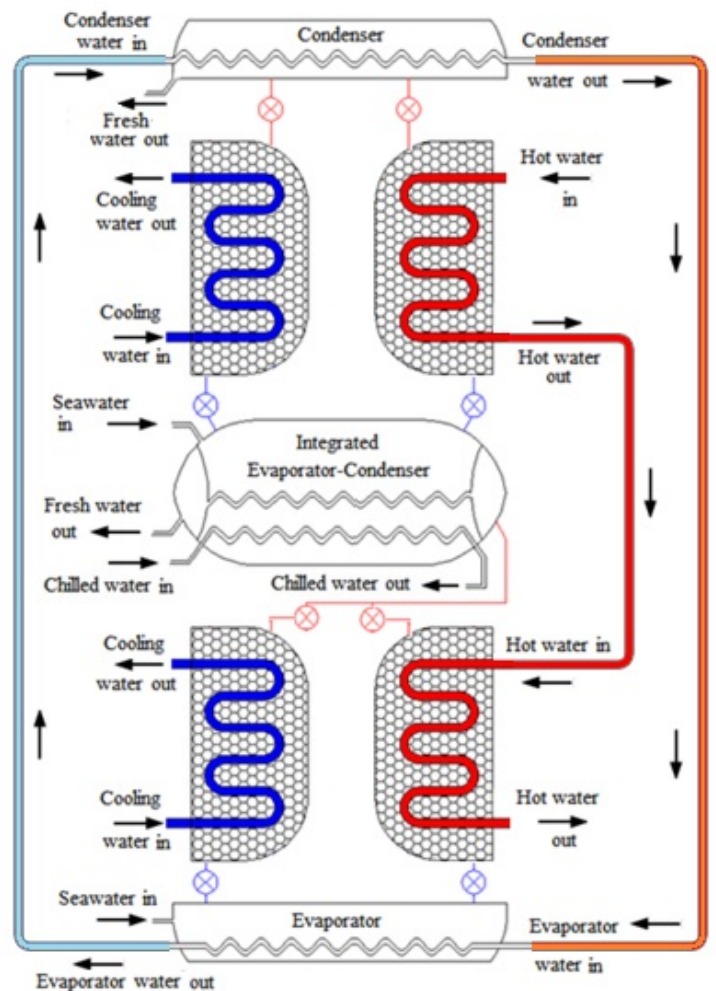
[a]   [b]
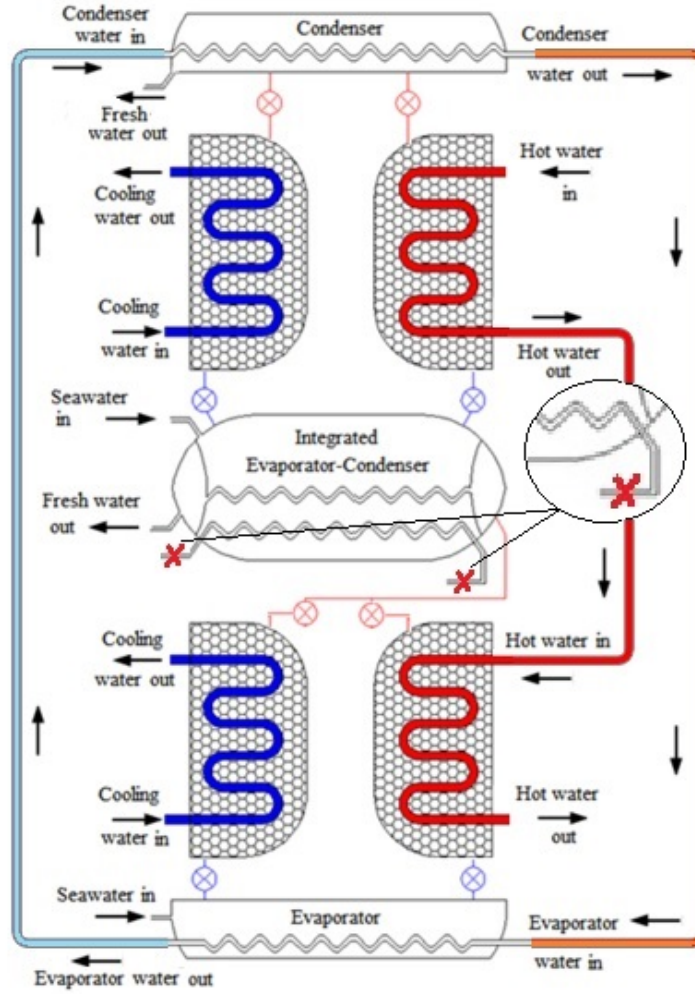
[c]

Fig. 3 Schematic diagram of the adsorption system at operating modes; 'A' (a), 'B' (b) and 'C' (c)

III. SYSTEM MODELLING

A full scale adsorption machine with the configuration presented in the previous section is simulated by Simulink to study its ability to produce mainly freshwater and cooling. All beds are packed with *AQSOA-Z02* with a capacity of 845 kg of adsorbent for each bed. In order to study the cycle, energy equations are solved for evaporator, condenser, integrated evaporator-condenser device, adsorber and desorber beds. In addition, water mass and salt concentration balance equations are solved for the evaporator and the integrated evaporator-condenser [13, 21] as shown in equations 1-12:

A. *Lower cycle, evaporator equations:*

Mass balance equation:

$$\frac{dM_{s,evap}}{dt} = \theta \dot{m}_{s,in} - \gamma \dot{m}_{brine} - \frac{dc_{ads}}{dt} M_a \tag{1}$$

Salt balance equation:

$$M_{s,evap}\frac{dX_{s,evap}}{dt} = \theta X_{s,in}\, \dot{m}_{s,in} - \gamma X_{s,evap}\, m_{brine} - X_D \frac{dc_{ads}}{dt}\, M_a \tag{2}$$

Energy balance equation:

$$\left[M_{s,evap}c_{p,s}\left(T_{evap},X_{s,evap}\right) + M_{HX,Evap}c_{p,HX}\right]\frac{dT_{evap}}{dt} = \theta.\, h_f\left(T_{evap},X_{s,evap}\right)\, \dot{m}_{s,in}$$

$$-h_{fg}(T_{evap})\frac{dc_{ads}}{dt}\, M_a$$

$$+\, \dot{m}_{chilled}c_p(T_{evap})\left(T_{chilled,in} - T_{chilled,out}\right)$$

$$-\gamma\, h_f\left(T_{evap},X_{s,evap}\right)\, m_{brine} \tag{3}$$

B. Integrated evaporator - condenser equations:

Mass balance equation:

$$\frac{dM_{s,evap-cond}}{dt} = \theta \dot{m}_{s,in} - \gamma m_{brine} - \frac{dc_{ads}}{dt}\, M_a \tag{4}$$

Salt balance equation:

$$M_{s,evap-cond}\frac{dX_{s,evap-cond}}{dt} = \theta X_{s,in}\, \dot{m}_{s,in} - \gamma X_{s,evap-cond}\, m_{brine} - X_D \frac{dc_{ads}}{dt}\, M_a \tag{5}$$

Evaporator side energy balance and wall equations:

$$\left[M_{s,evap}c_{p,s}\left(T_{evap},X_{s,evap}\right) + M_{HX,evap-cond}c_{p,HX}\right]\frac{dT_{evap}}{dt} =$$

$$\theta.\, h_f\left(T_{evap},X_{s,evap}\right)\, \dot{m}_{s,in}$$

$$-h_{fg}(T_{evap})\frac{dc_{ads}}{dt}\, M_a$$

$$+U_{evap-cond} \cdot A\left(T_{cond} - T_{evap}\right)$$

$$+\, \dot{m}_{chilled}c_p(T_{evap})\left(T_{chilled,in} - T_{chilled,out}\right)$$

$$-\gamma\, h_f\left(T_{evap},X_{s,evap}\right)\, m_{brine} \tag{6}$$

$$\left[M_{HX,evap-cond}c_{p,HX}\right]\frac{dT_{w-evap}}{dt} = h_{evap} \cdot A_{evap}\left(T_{w-evap} - T_{evap}\right) + \frac{2\pi kL}{ln\frac{r_1}{r_2}}\left(T_{w-cond} - T_{w-evap}\right) \tag{7}$$

Condenser side energy balance and wall equations:

$$\left[M_{cond}c_p(T_{cond}) + M_{HX,cond}c_{p,HX}\right]\frac{dT_{cond}}{dt} = -h_f(T_{cond})\frac{dM_d}{dt}$$

$$+h_{fg}(T_{cond})\frac{dc_{des}}{dt}\, M_a$$

$$-U_{evap-cond} \cdot A\left(T_{cond} - T_{evap}\right) \tag{8}$$

$$\left[M_{HX,evap-cond}c_{p,HX}\right]\frac{dT_{w-cond}}{dt} = h_{cond} \cdot A_{cond}\left(T_{cond} - T_{w-cond}\right) - \frac{2\pi kL}{ln\frac{r_1}{r_2}}\left(T_{w-cond} - T_{w-evap}\right)$$

$$\tag{9}$$

C. Upper cycle, condenser equation:

Energy balance equation:

$$\left[M_{cond}c_p(T_{cond}) + M_{HX,Cond}c_{p,HX}\right]\frac{dT_{cond}}{dt} = h_f\frac{dM_d}{dt} + h_{fg}(T_{cond})\, M_a\left(\frac{dc_{des}}{dt}\right)$$

$$+\, \dot{m}_{cond}c_p(T_{cond})\left(T_{cond,in} - T_{cond,out}\right) \tag{10}$$

202   **D. Upper and lower cycles beds equations:**

203

204   *Adsorption bed, energy balance equation:*

205    $$\left[M_a c_{p,a} + M_{HX} c_{p,HX} + M_{abe} c_{p,abe}\right]\frac{dT_{ads}}{dt} = z \cdot Q_{st} M_a \frac{dc_{ads}}{dt} - \dot{m}_{cw} c_p\left(T_{cw,out} - T"_{cw,in}\right) \tag{11}$$

206

207   *Desorption bed, energy balance equation:*

208    $$\left[M_a c_{p,a} + M_{HX} c_{p,HX} + M_{abe} c_{p,abe}\right]\frac{dT_{des}}{dt} = z \cdot Q_{st} M_a \frac{dc_{des}}{dt} + \dot{m}_{hw} c_p\left(T_{hw,in} - T"_{hw,out}\right) \tag{12}$$

209

210

211   Where, z is a flag equals 0 in heat recovery phase and 1 in all other cases.

212

213   As the cycle produces fresh water and cooling, three indicators can describe the cycle performance.
214   These indicators determine cycle productivity in terms of desalination, cooling and both. For desalination,
215   two parameters are calculated: specific daily water production (SDWP) and performance ratio (PR) which
216   is the ratio between heat of condensation to the heat of desorption. For cooling, two parameters are needed
217   which are specific cooling power (SCP) and coefficient of performance (COP). For the whole cycle
218   performance, overall conversion ratio (OCR) is calculated which is the ratio between useful effects
219   produced (summation of heat of condensation and heat of evaporation) over the input which is heat of
220   desorption [8, 13]. These parameters are calculated using equations 13-22:

221

222    $$SDWP = \int_0^{t_{cycle}} \frac{Q_{cond_{Top}} + Q_{cond_{Bottom}}}{(h_{fg}M_a)_{Top} + (h_{fg}M_a)_{Bottom}} dt \tag{13}$$

223    $$PR = \frac{1}{t_{cycle}}\int_0^{t_{cycle}} \frac{(m_d h_{fg})_{Top} + (m_d h_{fg})_{Bottom}}{Q_{Des_{Top}} + Q_{Des_{Bottom}}} dt \tag{14}$$

224    $$SCP = \int_0^{t_{cycle}} \frac{Q_{evap_{Top}} + Q_{evap_{Bottom}}}{M_{a_{Top}} + M_{a_{Bottom}}} dt \tag{15}$$

225    $$COP = \int_0^{t_{cycle}} \frac{Q_{evap_{Top}} + Q_{evap_{Bottom}}}{Q_{Des_{Top}} + Q_{Des_{Bottom}}} dt \tag{16}$$

226    $$OCR = \int_0^{t_{cycle}} \frac{Q_{evap_{Top}} + Q_{evap_{Bottom}} + Q_{cond_{Top}} + Q_{cond_{Bottom}}}{Q_{Des_{Top}} + Q_{Des_{Bottom}}} dt \tag{17}$$

227

228   *Where,*

229    $$Q_{cond_{Top}} = \dot{m}_{cond} c_p(T_{cond})\left(T_{cond,out} - T_{cond,in}\right) \tag{18}$$

230    $$Q_{cond_{Bottom}} = h_{cond} \cdot A_{cond}\left(T_{cond} - T_{w-cond}\right) \tag{19}$$

231

232    $$Q_{evap_{Top}} = h_{Evap} \cdot A_{Evap}\left(T_{w-evap} - T_{evap}\right) \tag{20}$$

233    $$Q_{evap_{Bottom}} = \dot{m}_{chilled} c_p(T_{evap})\left(T_{chilled,in} - T_{chilled,out}\right) \tag{21}$$

234

235    $$Q_{Des_{Top/Bottom}} = \dot{m}_{hw} c_p\left(T_{hw,in} - T_{hw,out}\right) \tag{22}$$

236

237   These set of energy, mass and salt balance equations are solved by Simulink. This model uses an
238   ODE45 solver which is Runge-Kutta technique with fifth-order method that performs a fourth-order
239   estimate of the error with variable time steps and relative tolerance of 10^{-3}. A lumped simulation model was
240   used where the adsorbent, adsorbate and heat exchangers are assumed to be momentarily at the same

temperature. Also perfect heat insulation is assumed for all parts. As stated before, the proposed system consists basically of two adsorption cycles with two beds in each. Validation of a 2 bed cycle has been presented by Youssef et al [11], with a maximum error within ±10%.

IV. ADSORBENT MATERIAL CHARACTERISTICS

AQSOA-Z02 is the SAPO-34 zeotype adsorbent material with a CHA-structure [22-24] where its linear formula is (SiO2)x(Al2O3)y(P2O5)z [25]. Adsorbent material adsorption characteristics are characterized by Adsorption isotherms and adsorption kinetics. Maximum amount of adsorbate that can be adsorbed per unit mass of dry material at a specific vapor pressure is represented by adsorption isotherms while adsorption kinetics are used to determine the rate of adsorption or desorption at the specified operating conditions.

For *AQSOA-Z02*, the water vapor uptake can be calculated using the model developed by Sun et al. [26] given by equations (23-24).

$$\frac{c}{c_{max}} = \frac{K(P/P_s)^m}{1+(K-1)(P/P_s)^m} \tag{23}$$

Where,
$$K = \alpha \, exp\big[m(Q_{st} - h_{fg})/RT\big] \tag{24}$$
$$\alpha = 9 * 10^{-7}, \, m = 3.18 \text{ and } Q_{st} = 3600 \, kJ/kg$$

Where, c_{max}, is maximum uptake, *m,* is heterogeneity factor, *h_{fg},* is the latent heat [kJ/kg], *R,* is universal gas constant [J/mol.K]

Adsorption kinetics are modeled by Linear driving force (LDF) model, (equations 25-26) [27].

$$\frac{dw}{dt} = k(w^* - w) \tag{25}$$
$$k = \left(15 \, D_{so}/R_p^2\right) e^{\left(\frac{-Ea}{RT}\right)} \tag{26}$$

To get the constants of the LDF model, tests using a dynamic vapor sorption (DVS) gravimetric analyzer were carried out by Youssef et al. [15]. These constants are presented in table III.

V. RESULTS AND DISCUSSION

In the adsorption cycle, the adsorbent material uptake depends on the partial pressure ratio which in turn depends on the evaporation and condensation temperatures. Figures 4 and 5 show the effect of evaporator and condenser water temperatures on the 2-bed cycle performance in terms of SDWP and SCP using different evaporator inlet water temperatures (10-30°C) and range of condenser inlet water temperatures (10-30°C). Cycle time is constant at 425 sec while beds heating and cooling water temperatures are 85°C and 30°C respectively. It is clear from these figures that water production and cooling are highly affected by condenser water temperature while evaporator water temperature has little effect. By lowering condenser water temperature, water production increases to reach 17.43 m^3/tonne adsorbent/day at 10°C condenser water temperature and 30°C evaporator water temperature. For condenser temperature of 30°C, the water production decreases to 6.68 m^3/tonne adsorbent/day while the cooling capacity decreases from 139.7 to 51.5 Rton/tonne adsorbent.
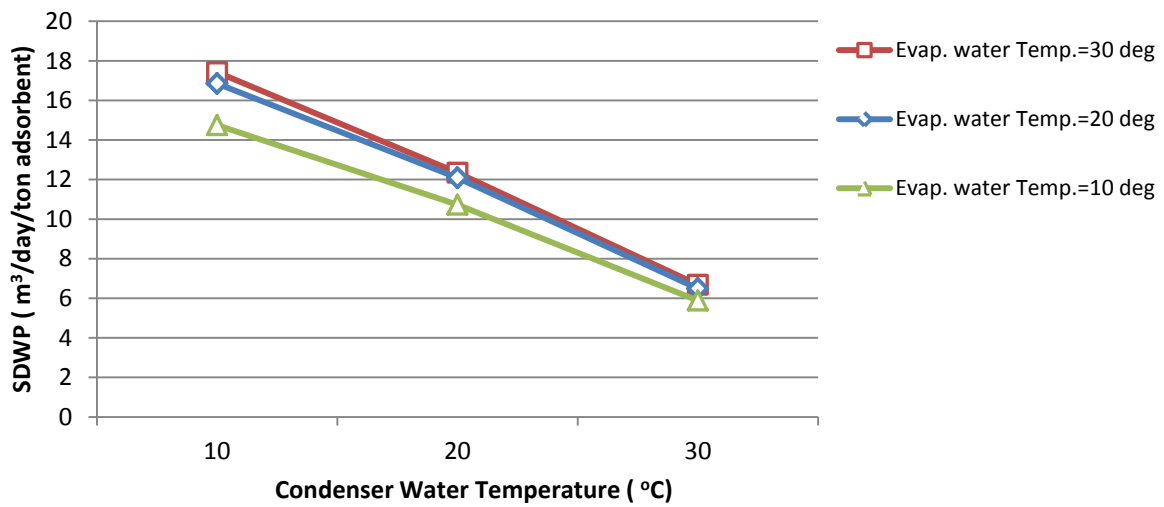
Fig. 4 SDWP at different condenser and evaporator water temperatures
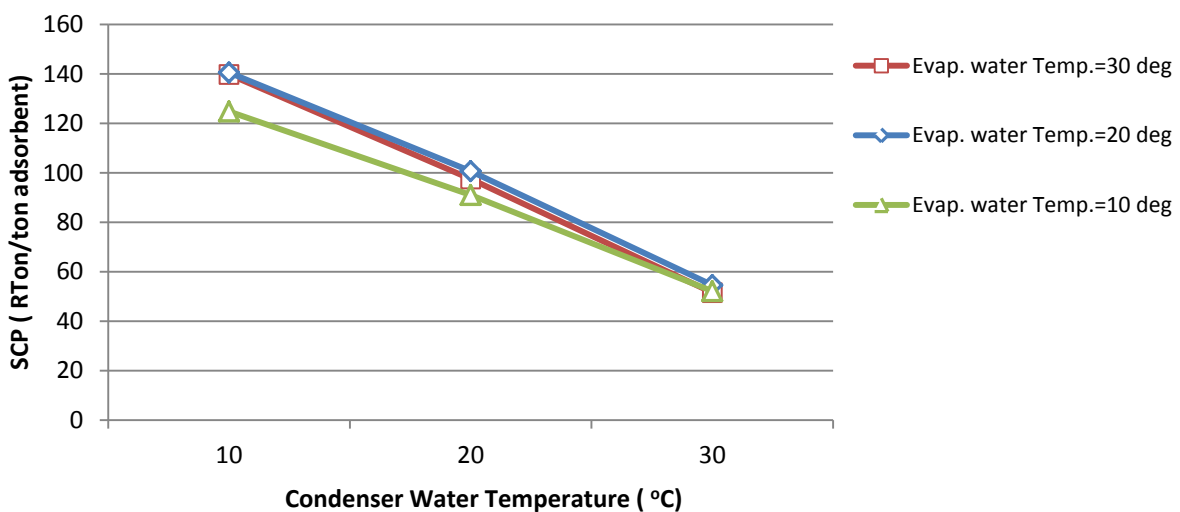
Fig. 5 SCP at different condenser and evaporator water temperatures

As highlighted earlier that decreasing condenser water temperature increases water production. In the proposed cycle described in section II, low condensing temperature can be achieved using the cooling effect produced at the evaporator of the lower cycle and the integrated evaporator/ condenser. Upper cycle condenser temperature is lowered by utilizing the cooling effect which is generated from lower cycle evaporator and in the integrated evaporator-condenser device, the lower cycle condenser temperature is reduced using low water temperature for upper cycle evaporator.

In the simulation, upper cycle beds heating and cooling inlet water temperatures are kept constant at 85°C and 30°C respectively. For lower cycle, beds heating water is the output from upper cycle desorbing bed while cooling water inlet temperature is kept constant at 30°C. Half cycle time is constant in all cases and equals to 425 sec divided into 400 sec of desorption/adsorption and 25 sec switching time.

Figure 6 compares the SDWP and SCP of the proposed system operating in mode A to those of the two bed conventional cycle [11] operating at condenser water temperature of 30°C and different evaporator water temperatures. In mode A, the lower cycle evaporator water inlet temperature ranged from 10 to 20°C. As shown in figure 6-a, the new cycle outperforms the 2-bed one at all lower evaporator inlet temperatures in terms of fresh water production (35% more) where 6.65 m^3/tonne adsorbent/day can be produced at 10°C lower evaporator water inlet temperature compared to 4.9 m^3/tonne adsorbent/day for the 2-bed cycle. In addition, at the same temperature cooling effect generated from the new cycle is 8.5% more as it reaches 46.6 Rton/tonne adsorbent while 2-bed cycle produces 43 Rton/tonne adsorbent. It appears from fig 6, that overall performance of the new cycle while operating at mode A is less affected by changing lower evaporator water inlet temperature. That is because upper and lower condensers water temperatures did not change by differing lower evaporator water temperature in addition to the shape of AQSOA-Z02 isotherm which yields nearly same water uptake at evaporator temperatures above 10°C (pressure ratio > 0.2) [26].

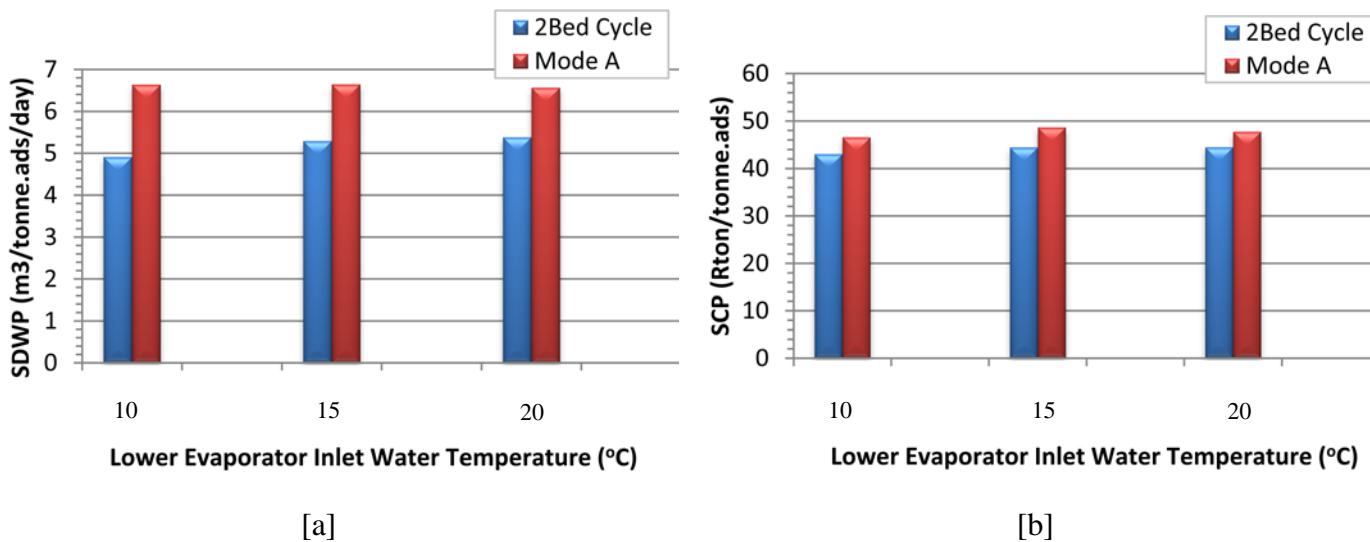[a]   [b]

Fig. 6 SDWP (a) & SCP (b) at different lower evaporator inlet water temperature, (mode 'A')

Figure 7 compares the performance of the proposed system operating at mode B to that of the 2-bed cycle at various upper cycle evaporator temperatures ranging from 5 to 20°C. As shown in figure 7-a, this operating mode produces water production three times (12.9 m^3/tonne adsorbent/day) that of the 2-bed (4.3 m^3/tonne adsorbent/day) cycle at temperature of 5°C. By increasing evaporator temperature, water production decreases in this operating mode but remains higher than the 2 bed cycle production at all

evaporator temperatures used. However, this increase in water production causes reduction in the output cooling capacity as shown in fig. 7-b. This is caused by utilizing all the cooling effect produced by the lower cycle evaporator for cooling the upper cycle condenser. Therefore, this operation mode is suitable for applications where water production is the primary need while cooling is a secondary product. However, the proportion of cooling capacity compared to the water production can be controlled by the evaporator cooling water temperature as shown in figures 7 a and b.

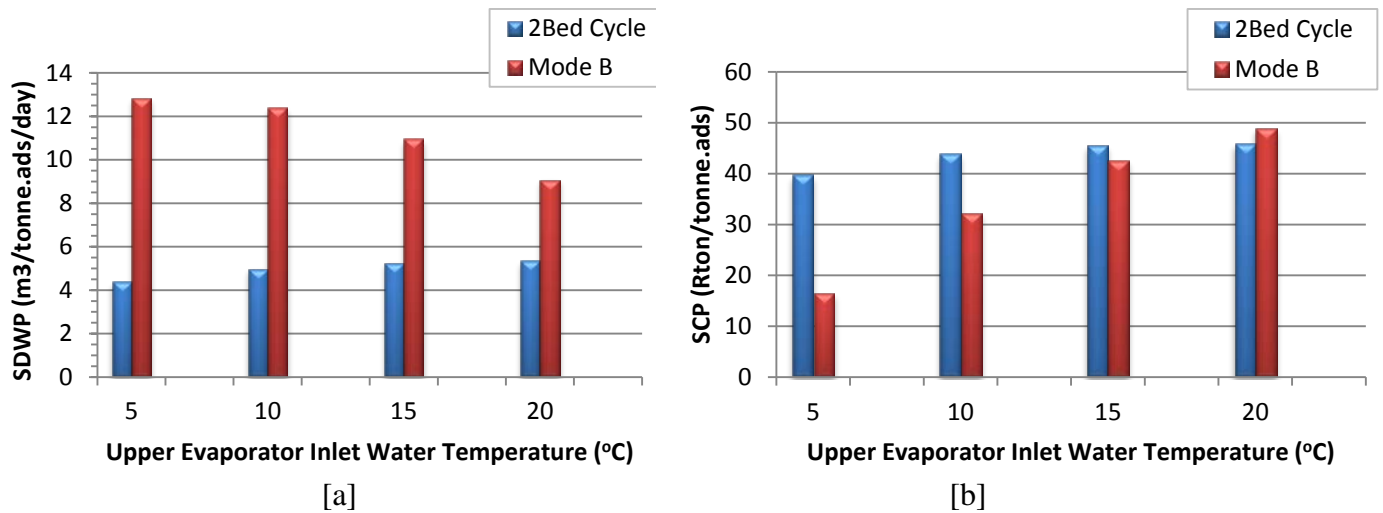[a]   [b]

Fig. 7 SDWP (a) & SCP (b) at different upper evaporator inlet water temperature with lower evaporator to upper condenser heat recovery, (mode 'B')

Figure 8 shows the water production from the proposed system operating at mode C where only desalinated water is produced with no cooling. It can be seen that the water production from the upper cycle is 18.87 m^3/tonne adsorbent/day while that of the lower cycle is 11.94 m^3/tonne adsorbent/day leading to an average overall water production of 15.41 m^3/tonne adsorbent/day. The high water production of the upper cycle is due to the lower condenser temperature achieved by the high cooling rate produced in the lower cycle evaporator. It is known that adsorption cycles performance depend on the achieved difference between maximum and lower uptakes, so by increasing adsorption pressure ratio and decreasing desorption pressure ratio, more difference in uptake is expected. Figure 9, illustrates how condenser temperature is affecting overall cycle performance through uptake. As shown in fig. 9, as condenser temperature decreases through modes 'A, B and C', desorption pressure ratio decreases as well which results in lower equilibrium uptake, i.e. higher desorbing rates and increased cycle outputs.
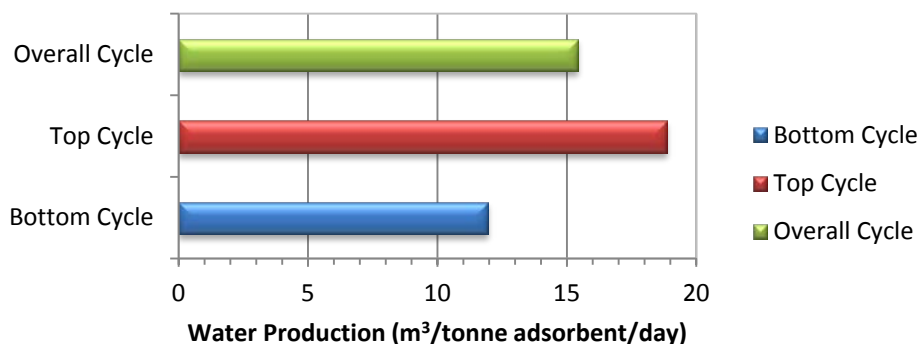

Fig. 8 SDWP in case of evaporator-condenser heat recovery with no cooling at upper evaporator, (mode 'C')
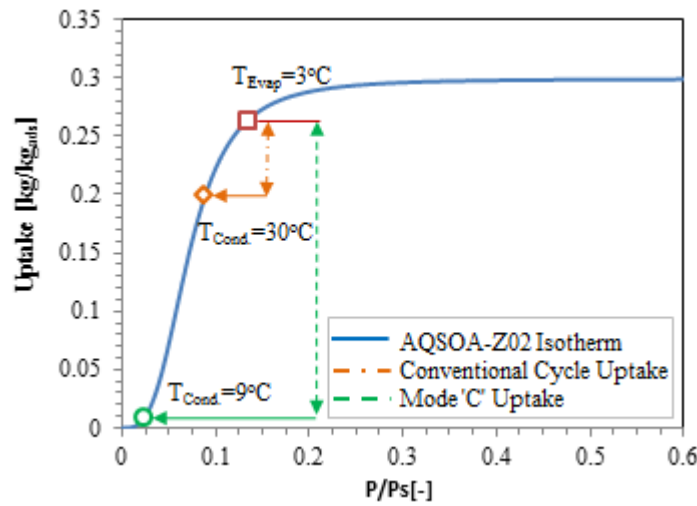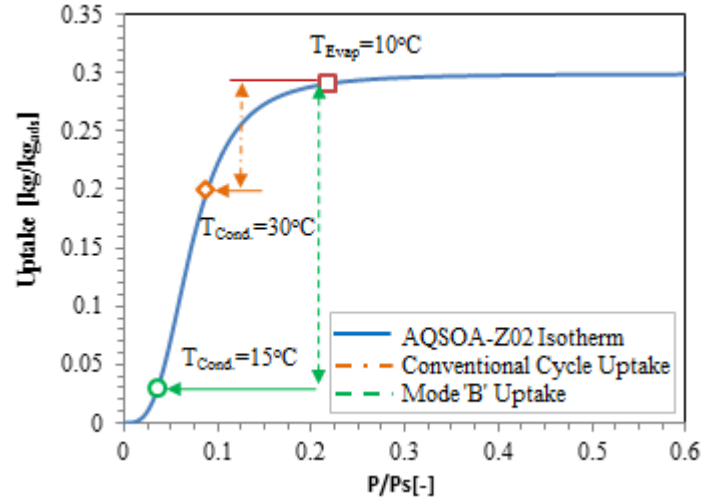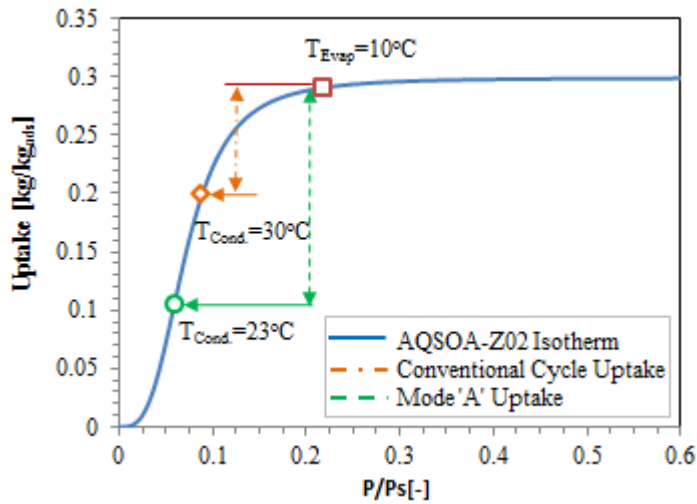
[a] 388 [b]

[c]

Fig. 9 (a, b and c) Comparison between conventional cycle uptake and proposed system uptake at different operating modes, 'A, B, and C' respectively.

Table IV summarizes the performance outputs of the proposed cycle at the three operating modes showing that mode 'C' produces the highest water production rate but with no cooling. Mode 'A' produces the highest cooling capacity but with lowest water production. As for mode 'B', its water production and cooling rate proportion can be controlled by the inlet evaporator water temperature. Outputs of modes 'A' and 'B' are comparable to those of previous data presented on 'table I' for Ng et al. [9], Mitra et al. [19, 20] and Youssef et al. [15] who presented in their work water and cooling production at low evaporator temperature below 20°C. It can be noticed that mode 'B' was able to produce 12.4 m^3/tonne/day while it ranged only from 1 to 6.2 m^3/tonne/day for previous researchers. When cooling is the main product, mode 'A' produced 46.6 Rton/tonne and 6.64 m^3/tonne/day while a 4-Bed system studied by Youssef et al. [15] resulted in 53.7 Rton/tonne and 6.2 m^3/tonne/day which is 13% higher in cooling but still less in water production. In case of mode 'C' when water is the only product, 15.4 m^3/tonne/day of water are produced from this system which are higher than Thu at al. [7, 17, 18] water production that ranged from 8.8 to 13.5

m3/tonne/day. Although the advanced cycle of Thu et al. [13] produced 26 m^3/tonne/day of water, it is still limited to water production only without any cooling production abilities due to cycle configuration and working at high evaporator temperature of 42^oC. The advantage of the proposed system compared to other systems is its flexibility as it is capable of working at different modes that can produce either water and cooling or water only which is not achievable by previous researchers work.

Figure 10 present OCR of the proposed system at operating modes 'A and 'B' with each column divided into PR and COP. When operating at mode 'A', fig. 10-a, the OCR at all evaporator water inlet temperatures is ranging from 0.665 to 0.685 while for 2-bed cycle it is nearly in the same range (0.683 to 0.7). However, for mode 'A', PR is higher at all temperatures. In mode 'B', fig. 10-b, as more water production is achieved, PR is greater than that of the 2-bed cycle as it reaches 0.51 compared to 0.3. However, the 2-bed cycle has higher COP than that of the new system at mode 'B' because more cooling is produced from the 2-bed cycle in this mode of operation. For mode C, results showed that PR is 0.64.

[a]   [b]
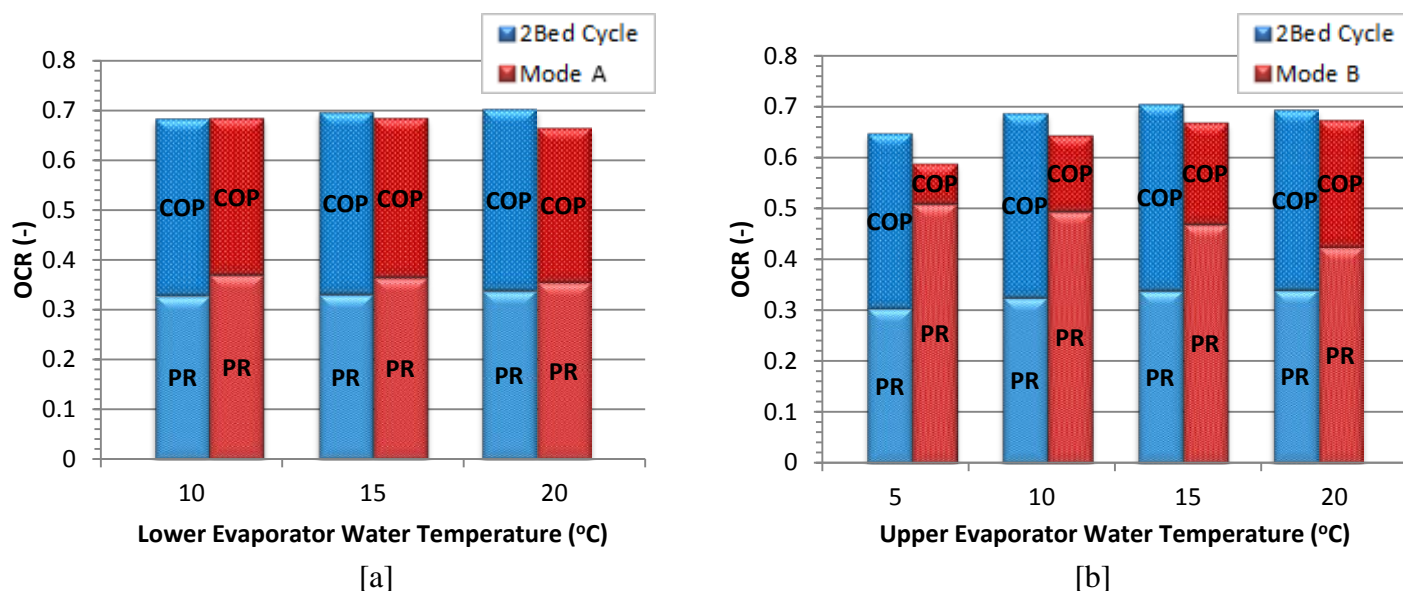
Fig. 10 OCR at different lower and upper evaporator inlet water temperature at modes A (a) and B (b)

As heating sources in this cycle comes from waste heat or solar energy, it is likely that the heating fluid temperature vary with time which could affect cycle performance. Figure 11 shows the effect of heat source temperature variations on cycle outputs for modes 'A' and 'B' at evaporator water temperature of 10^oC and for mode 'C'. It can be seen that by increasing or decreasing heat source temperature by 2 degrees, the cycle outputs will increase by 8% or decrease by 13%.
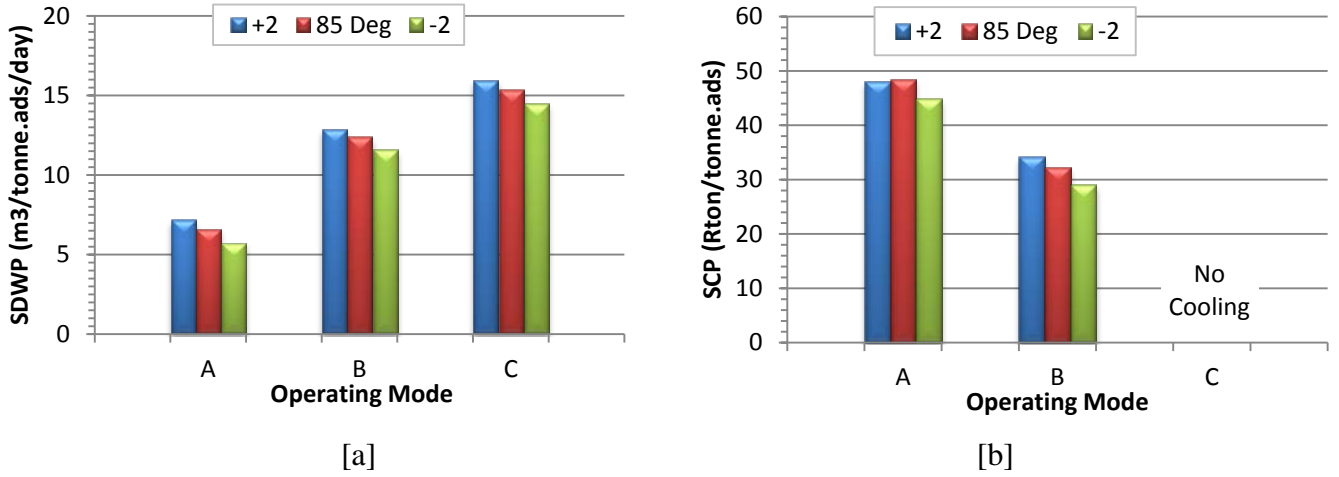
Fig. 11 Effect of hot source temperature variations on cycle outputs, SDWP (a) and SCP (b)

VI. ECONOMIC ANALYSIS

In this section, brief cost estimation is carried out for the proposed adsorption desalination and cooling system. Costs are classified as capital cost, running cost and maintenance cost. Adsorbent material, heat exchangers, pumps and control system components are examples of capital costs while thermal heat (if paid for), electricity and chemical treatment for feed and output water is deemed as running costs. Maintenance costs are considered when there are mechanical moving parts or any sort of filters that need to be replaced [28]. In this work, the cost analysis will be carried out based on the running cost of electricity consumption used for fluid pumping in the proposed cycle similar to the approach used by Thu et al. [28, 29]. Heating energy is assumed free of charge as it comes from either waste heat or solar energy [29] so it is not considered as part of running costs. Running costs are estimated using equations (27-35) which are based on water pumping energy consumption through desorbing/adsorbing beds, evaporator, condenser and integrated evaporator/condenser heat exchanger with an assumed pump efficiency (η_{pump}) of 85%.

$$\Delta h_f = \frac{f\,L\,v^2}{2\,g\,d} \tag{27}$$

Where Δh_f is the head loss, f is the friction factor, L is pipe length, v is water velocity in pipe and d is the inner pipe diameter.

$$PP_{elec.} = \frac{\Delta h_f \cdot g \cdot m^\cdot_{water}}{\eta_{pump}} \tag{28}$$

$$PP_{elec.-total} = PP_{Beds} + PP_{Lower\,Evap.} + \alpha.PP_{Upper\,Evap.} + PP_{Upper\,Cond.} \tag{29}$$

Where PP is the electric pumping power, α is a flag equal to 1 during mode 'B' and equal to 0 during modes 'A & C'.

After determining total electric power consumed in each operating mode, equations (30-31) are used to get portions of power (POP) needed to produce water and cooling which are necessary to calculate specific energy consumption for both products, eq. (32-33) and cost per unit product, eq. (34-35).

$$POP_{water} = \frac{Q_{cond.}}{Q_{cond.} + Q_{evap}} \tag{30}$$

$$POP_{cooling} = \frac{Q_{evap.}}{Q_{cond.} + Q_{evap}} \tag{31}$$

$$\text{Specific energy consumption}_{water} = \frac{POP_{water} \cdot PP_{elec.-total} \cdot 24}{SDWP \cdot M_a} \tag{32}$$

$$\text{Specific energy consumption}_{cooling} = \frac{POP_{cooling} \cdot PP_{elec.-total}}{SCP \cdot M_a} \tag{33}$$

$$Cost_{unit\ water} = \text{Specific energy consumption}_{water}\ x\ Energy\ rate_{elec.} \tag{34}$$

$$Cost_{unit\ cooling\ per\ day} = \text{Specific energy consumption}_{cooling}\ x\ Energy\ rate_{elec.}\ x\ 24 \tag{35}$$

As the results showed three modes of operation at different evaporator water temperatures, sample of cost estimation will be presented for each mode at 10^oC evaporator water temperature. Table V presents the production costs for water and cooling in the three operating modes 'A', 'B' and 'C' assuming electric energy cost rate of 0.144 US dollars/kWh [30]. It was found that water production cost reaches as low as 0.136 US$/m^3 at mode C which is comparable to the reported cost of 0.18 US$/m^3 [28]while cooling costs reached its minimum of 0.018US$/Rton.day at mode 'B'.

VII. CONCLUSIONS

The performance of a new multi-cycle adsorption desalination and cooling system using AQSOA-Z02 has been investigated and compared to a two bed conventional cycle. The system consists of two 2-adsorber bed cycles linked with integrated evaporator/condenser and can work at three different modes depending on desalinated water and cooling needs. It was found that decreasing condenser temperature upgrades cycle outputs of desalinated water and cooling therefore this proposed cycle outperforms conventional ones due to its ability to lower condenser temperature by utilizing part of the cooling effect produced from the evaporators. Comparing all modes at low evaporating temperature of 10^oC to the conventional 2-bed cycle concluded that mode 'A' increased water and cooling production by 35% and 8.5% respectively while mode 'B' raised water production rate by 250% but with a decrease in the cooling by 26%. Finally while no cooling is produced at mode 'C', maximum desalinated water output of 15.4 m^3/tonne adsorbent/day is achieved (314% higher than 2-bed cycle). Also, it was found that increasing the heat source temperature by 2^oC, will increase the cycle output by 8% while decreasing the heat source temperature 2^oC decrease the cycle output by 13% indicating that the system outputs are sensitive to changes in the heat source temperature. Furthermore, the average water production cost of this cycle is 0.15 US$/m^3 which is less than the reported value of 0.18 US$/m^3. This work highlights the potential of the

proposed multi cycle configuration with integrated evaporator/condenser to produce large amounts of desalinated water and cooling effect at low evaporator temperatures simultaneously with flexibility in proportion of water production and cooling outputs due to available operating modes.

Acknowledgment

REFERENCES

[1] K. C. Ng, B. B. Saha, A. Chakraborty, S. Koyama. Adsorption Desalination Quenches Global Thirst. Heat Transfer Engineering. 2008;29:845-8.

[2] H. T. El-Dessouky, H. M. Ettouney. Fundamentals of salt water desalination: ELSEVIER; 2002.

[3] P. G. Youssef, R. K. Al-Dadah, S. M. Mahmoud. Comparative Analysis of Desalination Technologies. Energy Procedia. 2014;61:2604-7.

[4] A. Asushi, C. Anutosh, G. Lizhen, K. Takao, K. S. C. O. K. Univ, N. K. Choon, S. B. Baran, W. X. Ling. Apparatus and method for desalination. Google Patents; 2006.

[5] J. W. Wu, E. J. Hu, M. J. Biggs. Thermodynamic analysis of an adsorption-based desalination cycle (part II): Effect of evaporator temperature on performance. Chemical Engineering Research and Design. 2011;89:2168-75.

[6] J. W. Wu, M. J. Biggs, P. Pendleton, A. Badalyan, E. J. Hu. Experimental implementation and validation of thermodynamic cycles of adsorption-based desalination. Applied Energy. 2012;98:190-7.

[7] K. Thu, K. C. Ng, B. B. Saha, A. Chakraborty, S. Koyama. Operational strategy of adsorption desalination systems. International Journal of Heat and Mass Transfer. 2009;52:1811-6.

[8] K. C. Ng, K. Thu, B. B. Saha, A. Chakraborty. Study on a waste heat-driven adsorption cooling cum desalination cycle. International Journal of Refrigeration. 2012;35:685-93.

[9] K. C. Ng, K. Thu, A. Chakraborty, B. B. Saha, W. G. Chun. Solar-assisted dual-effect adsorption cycle for the production of cooling effect and potable water. International Journal of Low-Carbon Technologies. 2009;4:61-7.

[10] P. G. Youssef, R. K. Al-Dadah, S. M. Mahmoud, H. J. Dakkama, A. Elsayed. Effect of Evaporator and Condenser Temperatures on the Performance of Adsorption Desalination Cooling Cycle. Energy Procedia. 2015;75:1464-9.

[11] P. G. Youssef, S. M. Mahmoud, R. K. Al-Dadah. Effect of Evaporator Temperature on the Performance of Water Desalination / Refrigeration Adsorption System Using AQSOA-ZO2. International Journal of Environment, Chemical, Ecological, Geological Engineering. 2015;9:679-83.

[12] K. C. A. Alam, A. Akahira, Y. Hamamoto, A. Akisawa, T. Kashiwagi. A four-bed mass recovery adsorption refrigeration cycle driven by low temperature waste/renewable heat source. Renewable Energy. 2004;29:1461-75.

[13] K. Thu, A. Chakraborty, Y.-D. Kim, A. Myat, B. B. Saha, K. C. Ng. Numerical simulation and performance investigation of an advanced adsorption desalination cycle. Desalination. 2013;308:209-18.

[14] K. Thu, A. Chakraborty, B. B. Saha, K. C. Ng. Thermo-physical properties of silica gel for adsorption desalination cycle. Applied Thermal Engineering. 2013;50:1596-602.

[15] P. G. Youssef, S. M. Mahmoud, R. K. Al-Dadah. Performance analysis of four bed adsorption water desalination/refrigeration system, comparison of AQSOA-Z02 to silica-gel. Desalination. 2015;375:100-7.

[16] A. Akahira, K. C. Amanul Alam, Y. Hamamoto, A. Akisawa, T. Kashiwagi. Mass recovery four-bed adsorption refrigeration cycle with energy cascading. Applied Thermal Engineering. 2005;25:1764-78.

[17] K. Thu, B. B. Saha, A. Chakraborty, W. G. Chun, K. C. Ng. Study on an advanced adsorption desalination cycle with evaporator–condenser heat recovery circuit. International Journal of Heat and Mass Transfer. 2011;54:43-51.

[18] K. Thu, H. Yanagi, B. B. Saha, K. C. Ng. Performance analysis of a low-temperature waste heat-driven adsorption desalination prototype. International Journal of Heat and Mass Transfer. 2013;65:662-9.

[19] S. Mitra, K. Srinivasan, P. Kumar, S. S. Murthy, P. Dutta. Solar Driven Adsorption Desalination System. Energy Procedia. 2014;49:2261-9.

[20] S. Mitra, P. Kumar, K. Srinivasan, P. Dutta. Performance evaluation of a two-stage silica gel + water adsorption based cooling-cum-desalination system. International Journal of Refrigeration. 2015.

[21] K. C. Ng, K. Thu, Y. Kim, A. Chakraborty, G. Amy. Adsorption desalination: An emerging low-cost thermal desalination method. Desalination. 2013;308:161-79.

[22] M. F. de Lange, K. J. F. M. Verouden, T. J. H. Vlugt, J. Gascon, F. Kapteijn. Adsorption-Driven Heat Pumps: The Potential of Metal–Organic Frameworks. Chemical Reviews. 2015;115:12205-50.

[23] D. TABATA, K. Okamoto, K. Taniguchi, S. KUBOKAWA. Adsorptive member and apparatus using the same. Google Patents; 2014.

[24] Database of zeolite structures. http://www.izastructure.org/databases/

[25] ACS Material SAPO-34 Data Sheet.2013,http://www.acsmaterial.com/product.asp?cid=72&id=80

[26] B. Sun, A. Chakraborty. Thermodynamic formalism of water uptakes on solid porous adsorbents for adsorption cooling applications. Applied Physics Letters. 2014;104:201901.

[27] H. T. Chua, K. C. Ng, A. Malek, T. Kashiwagi, A. Akisawa, B. B. Saha. Modeling the performance of two-bed, sillica gel-water adsorption chillers. International Journal of Refrigeration. 1999;22:194-204.

[28] K. Thu, A. Chakraborty, B. B. Saha, W. G. Chun, K. C. Ng. Life-cycle cost analysis of adsorption cycles for desalination. Desalination and Water Treatment. 2012;20:1-10.

[29] K. Thu. Adsorption desalination Theory and experiment: National University of Singapore; 2010.

[30] Electricity Rates Around the World.2015,http://www.worldatlas.com/articles/electricity-rates-around-the-world.html